

Lightcurves of the Karin family asteroids

Fumi Yoshida^a, Takashi Ito^{a,*}, Budi Dermawan^b, Tsuko Nakamura^c, Shigeru Takahashi^d,
Mansur A. Ibrahimov^e, Renu Malhotra^f, Wing-Huen Ip^g, Wen-Ping Chen^g, Yu Sawabe^h,
Masashige Haji^h, Ryoko Saito^h, Masanori Hirai^h

^a National Astronomical Observatory, Osawa 2-21-1, Mitaka, Tokyo, Japan

^b Department of Astronomy, Bandung Institute of Technology, Jalan Ganesha 10, Bandung 40132, Indonesia

^c Teikyo-Heisei University, 2-51-4 Higashi-Ikebukuro, Toshima, Tokyo 170-8445, Japan

^d Nobeyama Radio Observatory, Nobeyama 462-2, Minami-Maki-Mura, Nagano 384-1305, Japan

^e Ulugh Beg Astronomical Institute, 33 Astronomical Street, Tashkent 700052, Uzbekistan

^f Lunar & Planetary Laboratory, The University of Arizona, 1629 E. University Boulevard, Tucson, AZ 85721-0092, USA

^g Institute of Astronomy, National Central University, Jhongda Road 300, Jhongli, Taoyuan 32001, Taiwan

^h Fukuoka University of Education, Akama-Bunkyo-machi 1-1, Munakata, Fukuoka 811-4192, Japan

ARTICLE INFO

Article history:

Received 12 May 2012

Revised 25 November 2015

Accepted 6 January 2016

Available online 15 January 2016

Keywords:

Asteroids

Photometry

Rotation

ABSTRACT

The Karin family is a young asteroid family formed by an asteroid breakup 5.8 Myr ago. Since the members of this family probably have not experienced significant orbital or collisional evolution yet, it is possible that they still preserve properties of the original family-forming event in terms of their spin state. We carried out a series of photometric observations of the Karin family asteroids, and here we report on the analysis of the lightcurves including the rotation period of eleven members. The mean rotation rate of the Karin family members turned out to be much lower than those of near-Earth asteroids or small main belt asteroids (diameter $D < 12$ km), and even lower than that of large main belt asteroids ($D > 130$ km). We investigated a correlation between the peak-to-trough variation and the rotation period of the eleven Karin family asteroids, and found a possible trend that elongated members have lower spin rates, and less elongated members have higher spin rates. However, this trend has to be confirmed by another series of future observations.

© 2016 Elsevier Inc. All rights reserved.

1. Introduction

Asteroid families are remnants of catastrophic disruption and reaccumulation events between small bodies in the Solar System (e.g. Michel et al., 2003). Each member of an asteroid family has the potential to provide us with clues about the family-formation events that created them. However, since asteroid families are generally old (\sim Gyr), it is quite likely that the family members have undergone significant orbital, collisional, and spin-state evolution that masks properties of the original family-forming events.

A sophisticated numerical technique devised by Nesvorný et al. (2002) changed the above situation. Using their method, they detected three young asteroid families in the main belt: the Karin family (\sim 5.8 Myr old), the Iannini family (\sim 5 Myr old), and the Veritas family (\sim 8 Myr old). These families are remarkably younger than previously known asteroid families, and more and more younger asteroid clusters have been recognized since then (e.g.

Nesvorný and Vokrouhlický, 2006; Vokrouhlický and Nesvorný, 2008; 2009). With these discoveries in hand, we find many aspects of the study of young asteroid families interesting: their spin period distribution, their shape distribution, and possible detection of non-principal axis rotation.

We expect that the young family members preserve some properties of the original family-forming event in their spin period distribution. Although there are several laboratory experimental studies on the spin period distribution of collisional fragments (e.g. Fujiwara et al., 1989; Nakamura and Fujiwara, 1991; Kadono et al., 2009), it is hard to directly apply their results to real collisions between Small Solar System Bodies (SSSBs) in the gravity-dominant regime. Thus, observations of spin rates of the young asteroid family members can be unique opportunities to collect information on large-scale collisions.

As for the asteroid spin rate distribution, it is now widely known that the Yarkovsky–O'Keefe–Radzievskii–Paddack (YORP) effect may spin up or spin down 10-km-sized asteroids on a 10^8 yr timescale, and smaller asteroids could spin up/down even faster (e.g. Rubincam, 2000; Bottke et al., 2006). However, as the ages

* Corresponding author. Tel.: +81422343454; fax: +81422343840.

E-mail addresses: fumi.yoshida@nao.ac.jp (F. Yoshida), tito@cfca.nao.ac.jp (T. Ito).

of the young asteroid families are substantially shorter than the timescale of the YORP effect, each family member perhaps statistically retains its initial spin status just after the family-formation event. In old asteroid families, such as the Koronis family, the YORP effect has changed the initial spin rate since the family-formation events (e.g. [Slivan, 2002](#); [Slivan et al., 2003](#); [Vokrouhlický and Čapek, 2002](#); [Vokrouhlický et al., 2003](#)). Comparisons between the spin rate distribution of old and young asteroid families can serve as a help in the timescale estimate of the YORP effect. Actually the YORP effect is very sensitive to small-scale topography of asteroids (e.g. [Statler, 2009](#)). However, with the current observational data that we have in hand, we have not reached a detailed quantitative estimate of how seriously the YORP effect has influenced the dynamics of the Karin family members. Gaining a deeper understanding of these dynamics remains an aim of future inquiry.

In addition to the spin rate statistics, the shape distribution of the young asteroid family members is important for understanding the fragmentation and reaccumulation process of SSSBs in comparison with laboratory collisional experiments. It may help us understand the dynamical process of fragmentation and reaccumulation of asteroids, such as how angular momentum is distributed to each of the remnants. Also, it is possible to get an estimate of the satellite/binary forming efficiency at asteroid disruption events.

The young asteroid families also draw our attention in terms of possible detection of non-principal axis rotation (sometimes called “tumbling motion”). The study of a celestial body’s non-principal axis rotation gives us important insights into energy dissipation and excitation processes, as well as internal structure of the body. Non-principal axis rotation could be excited by collisions of small projectiles, but it will be damped quickly unless the excitation continues. This is the main reason why the non-principal axis rotation of SSSBs has been confirmed only for a few tens of lightcurves (e.g. [Harris, 1994](#); [Pravec and Harris, 2000](#); [Paolicchi et al., 2002](#); [Mueller et al., 2002](#); [Warner et al., 2009](#); [Oey et al., 2012](#); [Pravec et al., 2014](#)). However, the age of the young family asteroids is quite young, and we may be able to observe their non-principal axis rotation before it has totally decayed.

Based on the motivations mentioned above, we began a series of photometric observations of the young asteroid families in November 2002. In this paper we focus on the current result of our lightcurve observation of the Karin family asteroids through the R-band imaging that we had carried out until May 2004, and summarize the result for eleven Karin family members whose rotation period we determined. Note that throughout the present paper we assume that the lightcurve variations are due to shapes of asteroids, not due to albedo features.

2. Observations

During the period from November 2002 to May 2004, we observed and determined the rotational periods of eleven Karin family members, including the largest member, (832) Karin. [Table 1](#) shows the list of the observatories, the telescopes, and field of views of the instruments that we used for our observations.

We used the R-filter for our lightcurve observations because it is widely known that brightness of the reflected light in optical wavelengths from most asteroids becomes the highest in the R-band among the Johnson–Cousins *UBVRI* filters. In our observations all the telescopes were driven at the sidereal tracking rate, and the exposure time was limited by the moving rate of asteroids as well as by seeing during the observing nights. As typical main belt asteroids (MBAs) having the semimajor axis $a = 2.8$ AU move at the speed of $\sim 0.55''/\text{min}$ at its opposition, and as the typical seeing size at the observatories was from $1.0''$ to $3.0''$, we chose a single exposure time of two to eight minutes so that an asteroid has an appearance of a point source. Generally, we continued the R-band

Table 1

Observatories and instruments. E is the elevation of the observatory (m), D_t is the diameter of the telescope mirror that we used (m), and FOV denotes the field of view of the imaging system that we used for our purpose. The full observatory names and the telescope names are as follows: Steward: the 2.3 m telescope (“Bok”) at the Steward Observatory (Kitt Peak, Arizona, USA). Vatican: the 1.8 m telescope (“VATT”) at the Vatican Observatory (Mt. Graham, Arizona, USA). Maidanak: the 1.5 m telescope (“AZT”) at Maidanak Observatory (Uzbekistan). Lulin: the 1 m telescope at the Lulin Observatory (Taiwan). Kiso: the 1 m telescope at the Kiso Observatory (Nagano, Japan). Fukuoka: the 0.4 m telescope at the Fukuoka University of Education (Fukuoka, Japan).

Name	Longitude	Latitude	E	D_t	FOV
Steward	111°36′01.6″W	31°57′46.5″N	2071	2.29	4.5′ × 4.5′
Vatican	109°53′31.25″W	32°42′04.69″N	3191	1.8	6.8′ × 6.8′
Maidanak	66°53′47.08″E	38°40′23.95″N	2593	1.5	8.5′ × 3.5′
Lulin	120°52′25″E	23°28′07″N	2862	1.0	11.5′ × 11.2′
Kiso	137°37′42.2″E	35°47′38.7″N	1130	1.05	50′ × 50′
Fukuoka	130°35′44.7″E	33°48′45.3″N	70	0.40	5.75′ × 4.36′

imaging for a particular asteroid throughout a night except when we took images of standard stars: an “asteroid per night” strategy.

We used the Landolt standard stars ([Landolt, 1992](#)) for the purpose of calibration. Before and/or after each of the observing nights, we took dome flats or twilight sky flats for flat-fielding. After the observation, we applied a standard data reduction procedure against the data: bias subtraction and flat division. [Table 2](#) is the summary of our observational details.

3. Analysis and results

To construct composite lightcurves of asteroids from the observational data, we followed a sequence proposed by [Harris and Lupishko \(1989\)](#). The actual procedure is described in our previous publications ([Dermawan et al., 2002](#); [2011](#); [Yoshida et al., 2004](#)). Principally, it is an iterative repetition of frequency analysis and fitting to Fourier series. We employed two different algorithms to examine periodicities in the lightcurve data: Lomb’s Spectral Analysis (LSA, [Lomb, 1976](#)) and the WindowCLEAN Analysis (WCA, [Roberts et al., 1987](#)). WCA incorporates a discrete Fourier transform as well as the CLEAN algorithm ([Högbom, 1974](#)), and ([Mueller et al., 2002](#)) adopted WCA when they detected multiple rotational periodicities of asteroid (4179) Toutatis. When the frequency analysis is done, we fit the lightcurve with a Fourier series. We have to be particularly careful when we combine lightcurves derived from several observing runs because they generally have different lightcurve-mean magnitudes. See [Section 3.1](#) for details of how we combined the lightcurves obtained from multiple observing runs.

Once we have obtained the lightcurve of an asteroid, we estimate the peak-to-trough variation of its lightcurve. To compare the amplitudes (A) of the lightcurves of the Karin family members taken at different solar phase angles (α) with each other as well as with other solar system bodies, we used the empirical relationship by [Zappalà et al. \(1990\)](#) that normalizes the amplitudes to a solar phase angle of 0 degree. [Zappalà et al. \(1990\)](#) gives $A(\alpha) = A(0)(1 + m\alpha)$, and it empirically determines the parameter $m = 0.030$ for S-type asteroids, which the Karin family members are classified as. However, we have to note that these amplitudes can be only used in a statistical sense, because, except for (832) Karin, these asteroids’ spin obliquities are not known.

3.1. Procedure for combining lightcurves

In this subsection we describe how we dealt with the standard stars in our observation and how we combined lightcurves of asteroids obtained from different observing nights, making a single lightcurve for each asteroid.

Table 2

Aspect data of observed asteroids. Date of observations (mid-time of the observing night) in UT, ecliptic longitude λ (deg), ecliptic latitude β (deg), solar phase angle α (deg), and abbreviated codes of the observatories (S: Steward, V: Vatican, M: Maidanak, L: Lulin, K: Kiso, and F: Fukuoka), and the sky condition at the observational night (P: photometric, NP: non-photometric).

Date (UT)	λ	β	α	obs.	cond.
(832) Karin					
2003–08–22.64	330.7	1.6	0.85	F	P
2003–08–23.64	330.5	1.6	0.61	F	P
2003–09–03.63	328.2	1.6	4.70	F	P
2003–09–04.63	328.0	1.6	5.13	F	P
2003–09–05.63	327.8	1.6	5.54	K	NP
2003–09–26.19	324.8	1.5	13.36	V	P
2003–09–27.19	324.7	1.5	13.68	V	P
2003–09–28.17	324.6	1.5	13.99	V	P
2003–09–29.17	334.5	1.5	14.30	V	P
(7719) 1997 GT ₃₆					
2003–10–14.16	315.5	0.9	18.39	S	P
2003–10–15.15	315.6	0.9	18.53	S	P
2003–10–16.14	315.6	0.9	18.66	S	P
2003–10–17.14	315.7	0.8	18.79	S	P
(10783) 1991 RB ₉					
2004–03–24.50	236.6	1.7	14.94	S	P
2004–03–26.46	236.0	1.8	14.51	S	NP
2004–03–27.43	235.9	1.8	14.30	S	NP
2004–05–07.66	229.9	2.3	1.12	L	NP
2004–05–09.76	229.4	2.3	0.76	L	P
2004–05–10.68	229.2	2.3	0.83	L	P
2004–05–11.81	229.0	2.3	1.09	M	NP
2004–05–13.81	228.6	2.3	1.74	M	NP
(11728) Einer					
2003–05–08.44	251.9	3.0	8.57	V	P
2003–05–09.44	251.7	3.0	8.20	V	P
2003–06–29.62	242.3	2.1	11.97	L	P
2003–06–30.53	242.2	2.1	12.26	L	P
(13765) Nansmith					
2003–09–29.46	47.2	1.3	14.20	V	P
2003–10–15.38	45.1	1.4	8.53	S	P
2003–10–16.37	45.0	1.4	8.14	S	P
2003–10–17.37	44.8	1.4	7.73	S	P
2003–10–23.46	38.5	0.9	5.10	K	NP
2003–10–24.34	38.7	0.9	4.67	K	P
2003–10–26.42	39.2	0.9	3.80	K	NP
2003–10–27.43	39.4	0.9	3.36	K	NP
(16706) Svojsik					
2003–05–08.23	187.4	2.5	12.33	V	P
2003–05–09.30	187.3	2.5	12.63	V	P
(28271) 1999 CK ₁₆					
2002–11–17.69	64.7	–1.2	4.48	L	P
2002–12–01.71	64.6	–1.3	1.71	L	NP
2002–12–04.63	64.0	–1.3	2.95	L	P
2002–12–05.58	63.8	–1.3	3.36	L	P
2004–03–24.29	161.1	–1.3	7.81	S	P
2004–03–26.27	161.0	–1.2	8.56	S	NP
2004–03–27.22	160.6	–1.3	8.90	S	NP
(40921) 1999 TR ₁₇₁					
2003–07–20.71	300.5	–3.1	1.62	L	NP
2003–07–21.69	300.3	–3.1	1.37	L	NP
(43032) 1999 VR ₂₆					
2003–08–01.89	342.8	–4.3	12.14	M	P
2003–08–02.90	342.7	–4.3	11.79	M	P
2003–08–03.89	342.5	–4.3	11.44	M	P
2003–08–04.86	342.4	–4.3	11.10	M	P
2003–09–22.25	333.3	–4.2	9.32	V	P
2003–09–27.24	332.6	–4.1	11.12	V	P
2003–09–28.18	332.5	–4.1	11.44	V	P
2003–09–29.17	332.4	–4.1	11.78	V	P
(69880) 1998 SQ ₈₁					
2003–09–22.44	20.4	–1.7	7.72	V	P
2003–09–26.47	19.6	–1.8	6.10	V	P
2003–09–27.41	19.5	–1.8	5.71	V	P
2003–09–28.45	19.3	–1.8	5.28	V	P
2003–09–29.34	19.1	–1.9	4.90	V	P
2003–10–14.33	15.9	–2.0	1.84	S	P

(continued on next page)

Table 2 (continued)

Date (UT)	λ	β	α	obs.	cond.
(71031) 1999 XE ₆₈					
2003–09–01.87	353.2	–2.3	5.05	M	P
2003–09–02.86	353.0	–2.4	4.66	M	P
2003–09–03.85	352.8	–2.4	4.27	M	P
2003–09–26.34	348.1	–2.6	5.21	V	P
2003–09–28.27	347.7	–2.7	5.96	V	P

3.1.1. Observation of the Landolt standard stars

We took the following procedures when observing Landolt standard stars.

(1) *On photometric nights.* Before and/or after the observation of each asteroid, we take images of the Landolt standard stars at several different airmasses. We determine the atmospheric extinction coefficients of the night based on this dataset.

(2) *On non-photometric nights.* While we take images of asteroids, we take images of one or two Landolt standard stars, once or twice if possible, at the same airmasses at which we observed the asteroids.

3.1.2. Combining lightcurves I. (With clear maxima and minima)

When all the observations are done, we measure the brightness of asteroids by IRAF. Eventually we combine all the lightcurves from different observing nights into a single composite lightcurve for each asteroid.

(1) *Measuring field stars.* When we measure the brightness of an asteroid by IRAF, we also measure the brightness of five or six field stars that exist on the same image as the asteroid. Here we should note that all the field stars that we choose must be included in the USNO–A2.0 catalogue¹. Although we are aware that the brightness magnitude of the stars catalogued in the USNO–A2.0 catalog contains a certain degree of error, here we do not take care of the errors.

(2) *Elimination of anomalous field stars.* We draw lightcurves of each of the field stars, and confirm that none of those we have chosen is a variable star. Also, if any of the chosen field stars is located on an image frame with a serious problem such as caused by camera shutter problems or cosmic ray contamination, we discard the entire image itself from the analysis.

(3) *Choosing the brightest field star.* When we have found several field stars whose brightness does not vary with time, we select the brightest one among them as a comparison star for the asteroid's relative photometry. This is because errors in relative photometry are smaller when we choose a brighter star as a comparison star.

(4) *Relative photometry of asteroids.* Using the selected field stars as comparison stars, we carry out relative photometry work for each asteroid. As a result, we obtain lightcurves in relative magnitude for each of the observation nights for each of the asteroids.

(5) *Determination of lightcurve-mean magnitudes.* We determine lightcurve-mean magnitude of each asteroid from the lightcurves in relative magnitude. We get the lightcurve-mean magnitudes in the process of fitting each of the lightcurves with Fourier series. When we see maximum and minimum in lightcurves, determination of lightcurve-mean magnitude is straightforward.

¹ <http://tdc-www.harvard.edu/catalogs/ua2.html>.

Table 3

Major observational results. P is the rotation period (hours), $A(0)$ is the reduced peak-to-trough variation, α is the solar phase angle during our observation (deg), QC is the quality code of the period results, and the panel designation in Fig. 1. For (28271) 1999CK₁₆, * denotes the observation result in 2002, and † denotes the observation result in 2004. The \pm errors in P are derived from the stepsize of the CLEAN analysis.

Asteroid	P	$A(0)$	α	QC	Fig. 1
(832) Karin	18.348 ^{+0.037} _{-0.037}	0.56 \pm 0.02	0.6–14.3	2	a
(7719) 1997 GT ₃₆	29.555 ^{+0.031} _{-0.031}	0.31 \pm 0.02	18.4–18.8	2	b
(10783) 1991 RB ₉	7.334 ^{+0.005} _{-0.005}	0.26 \pm 0.02	0.8–14.9	3	c
(11728) Einer	13.622 ^{+0.150} _{-0.140}	0.14 \pm 0.01	8.6–12.3	2	d
(13765) Nansmith	10.526 ^{+0.014} _{-0.014}	0.06 \pm 0.02	7.7–17.7	2	e
(16706) Svojsik	5.866 ^{+0.120} _{-0.120}	0.09 \pm 0.04	12.3–13.2	1	f
(28271)* 1999 CK ₁₆	5.635 ^{+0.005} _{-0.010}	0.07 \pm 0.04	1.7–4.5	2	g
(28271)† 1999 CK ₁₆	5.645 ^{+0.043} _{-0.120}	0.17 \pm 0.02	7.8–8.9	2	h
(40921) 1999 TR ₁₇₁	6.662 ^{+0.043} _{-0.043}	0.35 \pm 0.02	1.4–1.6	2	i
(43032) 1999 VR ₂₆	32.890 ^{+0.078} _{-0.158}	0.60 \pm 0.06	9.3–12.1	2	j
(69880) 1998 SQ ₈₁	7.675 ^{+0.077} _{-0.014}	0.08 \pm 0.01	1.8–7.7	2	k
(71031) 1999 XE ₆₈	20.187 ^{+0.064} _{-0.064}	0.39 \pm 0.04	4.3–6.0	2	l

(6) *Combining lightcurves based on the lightcurve means.* When several observing nights are (nearly) consecutively distributed, we combine the lightcurves of each asteroid from all the observing nights, based on the lightcurve-mean magnitude that we have determined in Section 3.1.2 (5).

(7) *Frequency analysis.* For each asteroid, we carry out frequency analysis of the combined lightcurves produced in Section 3.1.2 (6) and get necessary quantities such as rotation period.

3.1.3. Combining lightcurves II. (Without clear maxima or minima)

When we do not see any maxima or minima in lightcurves of asteroids, determination of lightcurve-mean magnitude is not straightforward. This happens when the spin period of an asteroid is as long as, or longer than, the observational period—observation length of a night does not reach the spin period of an asteroid. In this case we utilize the observational data of the Landolt standard stars that we have prepared in Sections 3.1.1 (1) and 3.1.1 (2), and carry out the following procedures, instead of Sections 3.1.2 (5) and 3.1.2 (6), to combine several lightcurves of an asteroid into a single one. Note that we carry out the procedure described in this subsection only when the observation night is photometric. Observational data from non-photometric nights without clear maxima or minima is not used, and is just discarded.

(1) *Calibration of the field star brightness.* Using the Landolt standard stars, we calibrate the brightness of the field stars that we selected. Then we calculate the apparent brightness magnitude of the asteroid using the calibrated brightness of the field stars.

(2) *Combining lightcurves based on the lightcurve means.* Based on the magnitude of each of the asteroids estimated in Sections 3.1.3 (1), we combine their lightcurves from different nights into a single lightcurve.

(3) *Frequency analysis.* For each asteroid, we carry out frequency analysis of the combined lightcurves produced in Sections 3.1.3 (2), and get necessary quantities such as rotation period.

3.2. Lightcurves

Fig. 1 shows all the lightcurves that we obtained in the series of observations. Table 3 summarizes rotation period P , reduced peak-to-trough variation $A(0)$, solar phase angle α during the observation period, and the period quality code (Lagerkvist et al., 1989). As for the rotation period P , we chose the most reliable peak value

from the periodicity analysis results by LSA or WCA (mostly by WCA for the lightcurves presented in the present paper). We regard that the LSA analysis as compensating for vulnerabilities of WCA and justifying our result even when the lightcurve data contains large temporal gaps. Note that we checked out phase plots for the peaks of other periods, although we did not show them in the present paper.

Since Fig. 1 and Tables 2 and 3 describe most of our results, we just give supplementary information for three of the objects as follows:

(832) *Karin.* The results of our lightcurve observation of this asteroid are already published (Yoshida et al. (2004) for the observation in 2003, and Ito and Yoshida (2007) for the observation in 2004). Since our 2004 observation was mainly for multi-color photometry of this asteroid, here we just present our 2003 observation result from Yoshida et al. (2004).

(28271) 1999 CK₁₆. We observed this asteroid twice at two different oppositions: from November to December 2002 and in March 2004. The rotation periods that were derived from both the observations are close to each other. The lightcurve amplitudes taken in 2002 (Fig. 1(g)) and 2004 (Fig. 1(h)) are different because geometric configurations between the asteroid, observer, and the Sun were different.

(11728) *Einer.* The rotation period derived for this asteroid is from the most prominent peak obtained from the period analysis. However, note that other period values might also be possible due to potential aliasing.

4. Discussions

The spin period distribution of asteroids is often compared with the Maxwellian distribution (e.g. Binzel et al., 1989). Unfortunately, the number of our lightcurve samples is still far from being sufficient for such a detailed statistical discussion. Here, let us just compare the mean value of the rotation rate $1/P$ of the eleven Karin family asteroids that we observed with those of near-Earth asteroids (NEAs), small MBAs ($D < 12$ km), and large MBAs ($D > 130$ km). According to Table 2 of Binzel et al. (2002, p. 265), the mean values of the rotation rate of NEAs, small MBAs, and large MBAs are 4.80 ± 0.29 rev/day, 4.34 ± 0.23 rev/day, and 2.90 ± 0.12 rev/day, respectively. On the other hand, from our present work, the mean rotation rate of the Karin family asteroids turned out to be ~ 2.40 rev/day, or ~ 2.51 rev/day excluding (832) Karin (we used the period value obtained in 2004 for (28271) 1999CK₁₆). Therefore, the mean rotation rate of the Karin family members is much lower than those of the NEAs and the small MBAs, and even lower than that of the large MBAs. This may be quite an interesting fact, considering the widely believed hypothesis that most of the small MBAs are collisional remnants.

According to Table 2 of Binzel et al. (2002, p. 265), the reduced peak-to-trough variation of the NEAs, the small MBAs, and the large MBAs is 0.29, 0.28, and 0.19, respectively. Meanwhile, the average reduced peak-to-trough variation of the Karin family members is 0.24–0.27². The average value excluding (832) Karin, 0.24–0.25, is closer to that of the small MBA group with $D < 12$ km, rather than that of the large MBAs. This is consistent with our conventional knowledge that asteroid remnants, such as small MBAs or young family asteroids, are more likely to have an elongated

² It is ~ 0.26 if we choose the value 0.07 for (28271) 1999 CK₁₆, ~ 0.24 if we exclude (832) Karin and choose the value 0.07 for (28271) 1999 CK₁₆, ~ 0.27 if we choose the value 0.17 for (28271) 1999 CK₁₆, and ~ 0.25 if we exclude (832) Karin and choose the value 0.17 for (28271) 1999 CK₁₆.

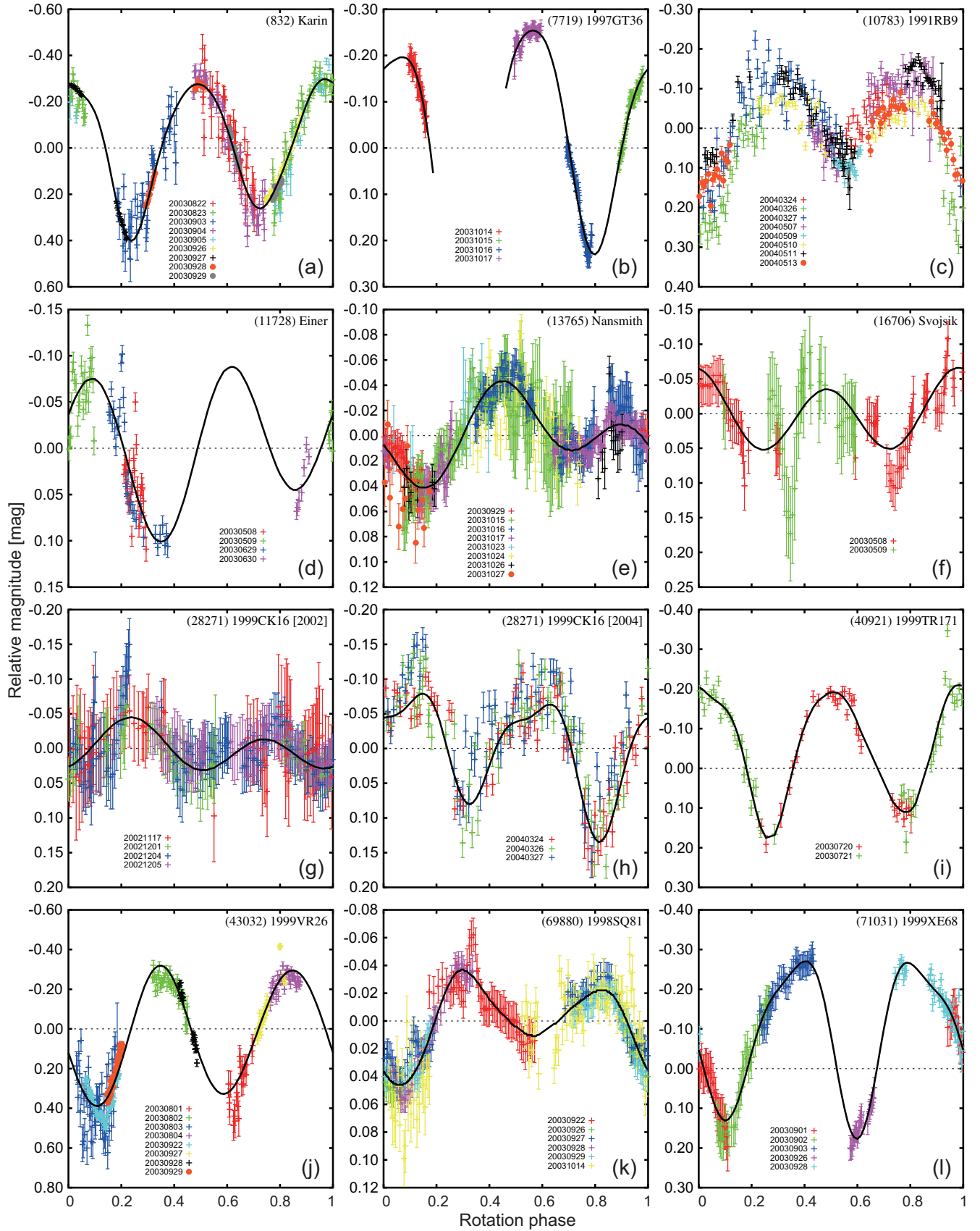


Fig. 1. Results of the lightcurve analysis of eleven Karin family asteroids. (a) (832) Karin, (b) (7719) 1997 GT₃₆, (c) (10783) 1991 RB₉, (d) (11728) Einer (e) (13765) Nansmith, (f) (16706) Svojsik, (g) (28271) 1999 CK₁₆ (observed in 2002), (h) (28271) 1999 CK₁₆ (observed in 2004), (i) (40921) 1999 TR₁₇₁, (j) (43032) 1999 VR₂₆, (k) (69880) 1998 SQ₈₁, and (l) (71031) 1999 XE₆₈. The vertical axis denotes the relative magnitude referred to a field star at each observing night. Note that the lightcurve of (832) Karin in (a) is a quoted one from Yoshida et al. (2004).

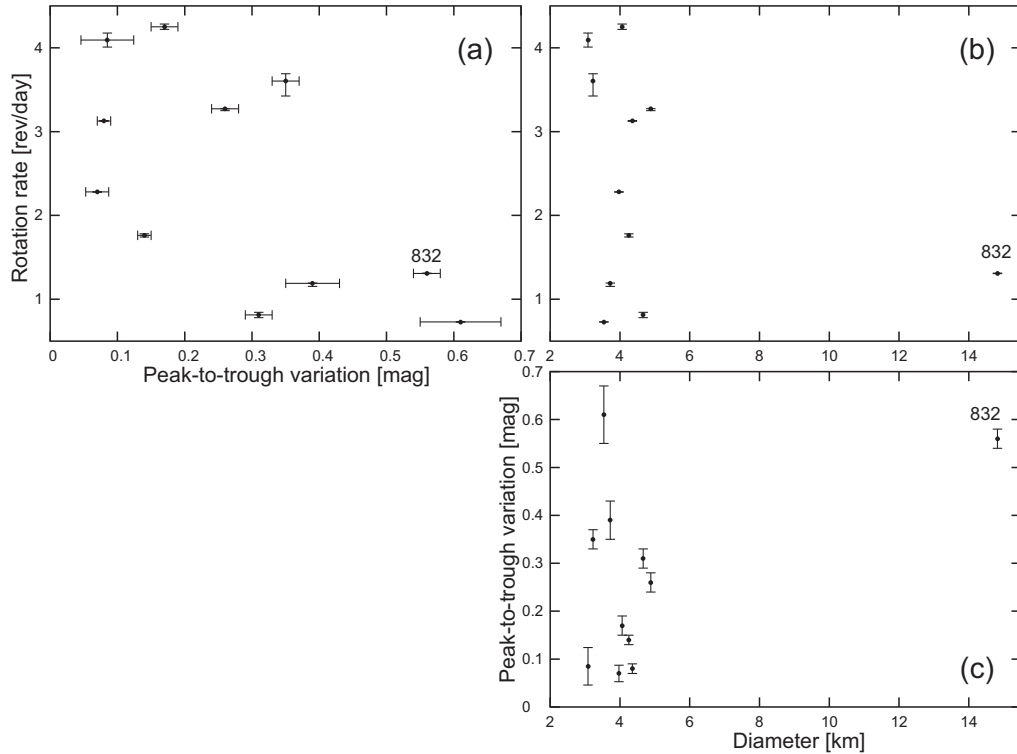


Fig. 2. Relation between the rotation rate $1/P$, diameter D , and the reduced peak-to-trough variation $A(0)$ of the eleven Karin family asteroids that we observed. (a) $A(0)$ and $1/P$, (b) D and $1/P$, and (c) D and $A(0)$. The largest member, (832) Karin, is denoted as “832”. Note that as for (28271) 1999 CK₁₆ we used its values obtained from our 2004 observation, as its $A(0)$ value in 2004 is larger than its value in 2002, being closer to their maximum.

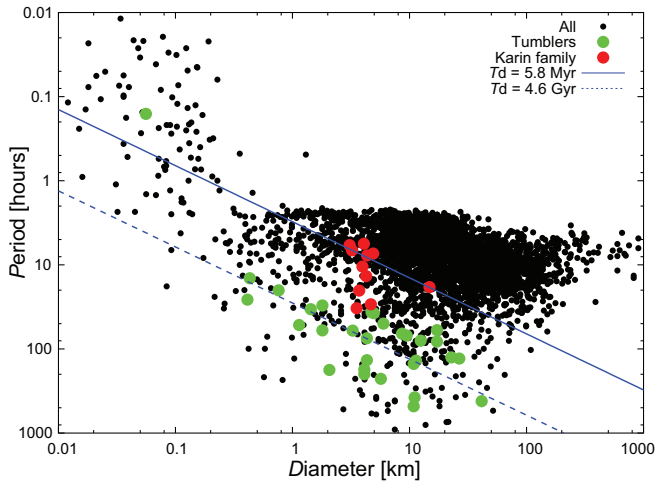


Fig. 3. Relation between the rotation period P (hours) and diameter D (km) of 3,745 known asteroids (filled black circles) including 31 tumblers (filled green circles) and the eleven Karin family asteroids (filled red circles). The diagonal blue lines show the theoretical (D, P) relation of asteroids when their damping timescale $T_d = 5.8$ Myr (the upper solid blue line) and when their damping timescale $T_d = 4.6$ Gyr (the lower dashed blue line) calculated by Eq. (1). (For interpretation of the references to color in this figure legend, the reader is referred to the web version of this article).

(and irregular) shape than a spherical shape compared with large asteroids that can be parent bodies of asteroid families.

We summarized our main result of the spin period P and the peak-to-trough variation magnitude $A(0)$ of the eleven Karin family members in Fig. 2 (we are aware that we have ignored the effect of asteroids’ obliquity in this figure, because we have no information on it so far). In Fig. 2(a) that shows the relation between $A(0)$ and $1/P$, you may see a slight trend from the top left to the

bottom right, which tells us that elongated asteroids have a lower spin rate, and those less elongated asteroids have a higher spin rate. A similar trend has been recognized in fast-rotating sub-km-size MBAs (Dermawan et al., 2011; Nakamura et al., 2011). However, we are aware that the number of our present lightcurve samples is not large enough to reach a definite conclusion on our conjecture. In other words, Fig. 2(a) may be just a scatter plot from the fact that the number of objects is not large enough for rigorously statistical discussions. Whether the “trend” really exists depends on how many more lightcurve samples of the Karin family members we can obtain from now on.

At the end of this paper, we would like to consider the possibility that some of the Karin family members still possess non-principal axis rotation. From the result that we have presented in the previous sections, we plotted the rotation period of the eleven Karin family asteroids on a diagram that shows the relation between rotation period P and diameter D in Fig. 3. For this figure, we estimated the diameter of the Karin family members from its absolute magnitude H using the relationship $\log_{10} D = 3.1295 - 0.5 \log_{10} p - 0.2H$ where p is the albedo of an asteroid (Bowell and Lumme, 1979). We used the absolute magnitude values of the asteroids listed on the Lowell asteroid orbital elements database³. We assumed the albedo value of $p = 0.21$ for the S-type asteroids (cf. Yoshida and Nakamura, 2007; Strom et al., 2015)⁴.

³ <ftp://ftp.lowell.edu/pub/elgb/astorb.html>.

⁴ The value $p = 0.21$ is the mean albedo calculated from the catalog of asteroid albedo and taxonomic types in PSI PDS database, <http://sbn.psi.edu/pds/resource/albedo.html>. The albedo value can be dependent on asteroid size, but we are not sure how strongly or weakly dependent it is. For example, recent survey observations have revealed the albedo dependence on asteroid size for each of the taxonomic types (e.g. Usui et al., 2013). In Usui et al.’s (2013) Fig. 5(b) for S-type asteroids, we may (or may not) see some skewed albedo distribution in the diameter range of $D < 10$ km, but we are not sure about the quantitative analysis result in a smaller range. Another thing is that the range of D of the asteroids that we

For comparison, we also plotted the (D, P) relation of 3,745 known asteroids listed on the PSI PDS lightcurve database whose rotational periods are known to a certain reliability⁵. For these asteroids, we applied the mean albedo of $p = 0.081$ following Ryan and Woodward (2010) to all the asteroids, assuming their absolute magnitude H listed in the Lowell asteroid orbital elements database mentioned above. Also, among these asteroids we highlighted 31 possible tumblers⁶ in green so that we can compare their (D, P) relation with that of the Karin family asteroids.

Theoretically, the damping timescale of the non-principal axis rotation of a celestial body T_d (Gyr) can be expressed in its relationship between P (hours) and D (km) as in the following equation by Harris (1994), a reconsideration of a theory by Burns and Safronov (1973):

$$P \sim 17D^{\frac{2}{3}} T_d^{\frac{1}{3}}. \quad (1)$$

Smaller and slower rotators have longer damping timescales of the non-principal axis rotation. In Fig. 3 we drew two damping timescales of non-principal axis rotation using diagonal lines calculated by Eq. (1). The upper solid blue line in Fig. 3 indicates the (D, P) relation of asteroids when their damping timescale $T_d = 5.8$ Myr, equivalent to the age of the Karin family. The lower dashed blue line in Fig. 3 indicates that of asteroids when their damping timescale $T_d = 4.6$ Gyr, almost equivalent to the age of the solar system. You can see from Fig. 3 that many of the Karin members we observed are located below the upper solid line for $T_d = 5.8$ Myr, indicating that they can still maintain the non-principal axis rotation, if there is any, since their damping timescale T_d is possibly longer than their age, 5.8 Myr. Although in the present analysis we did not detect clues on the non-principal axis rotation of the Karin family members, several members with relatively long rotational periods such as (7719) 1997 GT₃₆, (43032) 1999 VR₂₆, or (71031) 1999 XE₆₈ are still candidates as tumbling asteroids.

We greatly appreciate the effort and courtesy extended by all the people who helped us during our observations at the Vatican Observatory's "VATT" (the Alice P. Lennon Telescope and the Thomas J. Bannan Astrophysics Facility). We thank Elizabeth Green, Paula White, Ed Olszewski, and Andy Odell for allowing our use of the Steward 90-inch "Bok" telescope. FY is deeply thankful to Tom Gehrels who recommended that we use the VATT and the Bok telescopes in Arizona, and particularly for his encouragement of our observing activity and his enormous contribution to asteroid studies. Without his warmth, help, and thoughtful suggestions, we could not have carried out our observations there at all. The staff members at the Maidanak Observatory greatly helped us during our stay and observing activity. The authors thank the two anonymous referees for suggesting directions that significantly improved the quality of this paper. FY also has benefited from stimulating enlightenment by Murier Yoshida. Detailed and constructive review by Yolande McLean has considerably improved the English presentation of this paper. Some part of the data analysis was performed at the National Astronomical Observatory of Japan's Astronomy Data Center (ADC) and Center for Computational Astrophysics (CfCA). This study is supported by the JSPS Kakenhi grant (16740259/2004–2005, 18540426/2006–2008, 18540427/2006–2008, 21540442/2009–2011, 25400458/2013–2015,

25400238/2013–2015), the JSPS program for Asia–Africa academic platform (2009–2011), the JSPS bilateral open partnership joint research project (2014–2015), the Sumitomo Foundation research funding (030755/2003–2004), and the Heiwa Nakajima Foundation research funding for Asian studies (2009).

References

- Binzel, R.P., Farinella, P., Zappalà, V., et al., 1989. Asteroid rotation rates: Distributions and statistics. In: Binzel, R.P., Gehrels, T., Matthews, M.S. (Eds.), *Asteroids II*. The University of Arizona Press, Tucson, Arizona, pp. 416–441.
- Binzel, R.P., Lupishko, D.F., Di Martino, M., et al., 2002. Physical properties of near-Earth objects. In: Bottke, W.F., Cellino, A., Paolicchi, P., Binzel, R.P. (Eds.), *Asteroids III*. The University of Arizona Press, Tucson, Arizona, pp. 255–271.
- Bottke, W.F., Nesvorný, D., Rubincam, D.P., et al., 2006. The Yarkovsky and YORP effects: Implications for asteroid dynamics. *Annu. Rev. Earth Planet. Sci.* 34, 157–191.
- Bowell, E., Lumme, K., 1979. Colorimetry and magnitudes of asteroids. In: Gehrels, T. (Ed.), *Asteroids*. The University of Arizona Press, Tucson, Arizona, pp. 132–169.
- Burns, J.A., Safronov, V.S., 1973. Asteroid nutation angles. *Mon. Not. R. Astron. Soc.* 165, 403–411.
- Dermawan, B., Nakamura, T., Fukushima, H., et al., 2002. CCD photometry of the MUSES-c mission target: Asteroid (25143) 1998 SF₃₆. *Publ. Astron. Soc. Japan* 54, 635–640.
- Dermawan, B., Nakamura, T., Yoshida, F., 2011. Subaru lightcurve observations of sub-km-sized main-belt asteroids. *Publ. Astron. Soc. Japan* 63, S555–S576.
- Fujiwara, A., Cerroni, P., Davis, D.R., et al., 1989. Experiments and scaling laws for catastrophic collisions. In: Binzel, R.P., Gehrels, T., Matthews, M. (Eds.), *Asteroids II*. The University of Arizona Press, Tucson, Arizona, pp. 240–265.
- Harris, A.W., 1994. Tumbling asteroids. *Icarus* 107, 209–211.
- Harris, A.W., Lupishko, D.F., 1989. Photometric lightcurve observations and reduction techniques. In: Binzel, R.P., Gehrels, T., Matthews, M.S. (Eds.), *Asteroids II*. The University of Arizona Press, Tucson, Arizona, pp. 39–53.
- Högbom, J.A., 1974. Aperture synthesis with a non-regular distribution of interferometer baselines. *Astron. Astrophys. Suppl. Ser.* 14, 417–426.
- Ito, T., Yoshida, F., 2007. Color variation of a very young asteroid, karin. *Publ. Astron. Soc. Japan* 59, 269–275.
- Kadono, T., Arakawa, M., Ito, T., et al., 2009. Spin rates of fast-rotating asteroids and fragments in impact disruption. *Icarus* 200, 694–697.
- Lagerkvist, C.I., Harris, A.W., Zappalà, V., 1989. Asteroid lightcurve parameters. In: Binzel, R.P., Gehrels, T., Matthews, M.S. (Eds.), *Asteroids II*. The University of Arizona Press, Tucson, Arizona, pp. 1162–1179.
- Landolt, A.U., 1992. UBVR photometric standard stars in the magnitude range 11.5–16.0 around the celestial equator. *Astron. J.* 104, 340–371, 436–491.
- Lomb, N.R., 1976. Least-squares frequency analysis of unequally spaced data. *Astrophys. Space Sci.* 39, 447–462.
- Michel, P., Benz, W., Richardson, D.C., 2003. Disruption of fragmented parent bodies as the origin of asteroid families. *Nature* 421, 608–611.
- Mueller, B.E.A., Samarasinha, N.H., Michael, M.J.S., 2002. The diagnosis of complex rotation in the lightcurve of 4179 toutatis and potential applications to other asteroids and bare cometary nuclei. *Icarus* 158, 205–311.
- Nakamura, A., Fujiwara, A., 1991. Velocity distribution of fragments formed in a simulated collisional disruption. *Icarus* 92, 132–146.
- Nakamura, T., Dermawan, B., Yoshida, F., 2011. Sphericity preference in shapes of sub-km-sized fast-rotating main-belt asteroids. *Publ. Astron. Soc. Japan* 63, S577–S584.
- Nesvorný, D., Bottke, W.F., Dones, L., et al., 2002. The recent breakup of an asteroid in the main-belt region. *Nature* 417, 720–722.
- Nesvorný, D., Vokrouhlický, D., 2006. New candidates for recent asteroid breakups. *Astron. J.* 132, 1950–1958.
- Oey, J., Pilcher, F., Benishek, V., et al., 2012. Photometric analysis of the very long period and tumbling asteroid 1278 kenya. *Minor Planet Bull.* 39, 86–88.
- Paolicchi, P., Burns, J.A., Weidenschilling, S.J., 2002. Side effects of collisions: spin rate changes, tumbling rotation states, and binary asteroids. In: Bottke, W.F., Cellino, A., Paolicchi, P., Binzel, R.P. (Eds.), *Asteroids III*. The University of Arizona Press, Tucson, Arizona, pp. 517–526.
- Pravec, P., Harris, A.W., 2000. Fast and slow rotation of asteroids. *Icarus* 148, 12–20.
- Pravec, P., Scheirich, P., Ďurech, J., et al., 2014. The tumbling spin state of (99942) apophis. *Icarus* 233, 48–60.
- Roberts, D.H., Lehar, J., Dreher, J.W., 1987. Time series analysis with CLEAN I. derivation of a spectrum. *Astron. J.* 93, 968–989.
- Rubincam, D.P., 2000. Radiative spin-up and spin-down of small asteroids. *Icarus* 148, 2–11.
- Ryan, E.R., Woodward, C.E., 2010. Rectified asteroid albedos and diameters from IRAS and MSX photometry catalogs. *Astron. J.* 140, 933–943.
- Sivan, S.M., 2002. Spin vector alignment of koronis family asteroids. *Nature* 419, 49–51.
- Slivan, S.M., Binzel, R.P., Crespo da Silva, L.D., et al., 2003. Spin vectors in the Koronis family: Comprehensive results from two independent analyses of 213 rotation lightcurves. *Icarus* 162, 285–307.
- Statler, T.S., 2009. Extreme sensitivity of the YORP effect to small-scale topography. *Icarus* 202, 502–513.

observed this time is rather narrow (see Fig. 2(c)) except (832) Karin, and we can expect that the albedos for these asteroids are not so different from each other, even if there is a dependency of albedo on size. Therefore, in the present paper, we used the average albedo.

⁵ <http://sbn.psi.edu/pds/resource/lc.html> as of April 30, 2012 (V12.0). Among the lightcurve datafile data/lc_summary.tab, we selected the asteroids only with the lightcurve reliability of 2, 2+, 3 or higher.

⁶ Among all the lightcurve data in data/lc_summary.tab, we selected the asteroids having the credible tumbling flag T or T+.

- Strom, R.G., Malhotra, R., Xiao, Z., et al., 2015. The inner solar system cratering record and the evolution of impactor populations. *Res. Astron. Astrophys.* 15, 407–434.
- Usui, F., Kasuga, T., Hasegawa, S., et al., 2013. Albedo properties of main belt asteroids based on the all-sky survey of the infrared astronomical satellite *akari*. *Astrophys. J.* 762, 56.
- Vokrouhlický, D., Nesvorný, D., 2008. Pairs of asteroids probably of a common origin. *Astron. J.* 136, 280–290.
- Vokrouhlický, D., Nesvorný, D., 2009. The common roots of asteroids (6070) rhainland and (54827) 2001 NQ8. *Astron. J.* 137, 111–117.
- Vokrouhlický, D., Nesvorný, D., Bottke, W.F., 2003. The vector alignments of asteroid spins by thermal torques. *Nature* 425, 147–151.
- Vokrouhlický, D., Čapek, D., 2002. YORP-induced long-term evolution of the spin state of small asteroids and meteoroids: Rubincam's approximation. *Icarus* 159, 449–467.
- Warner, B.D., Harris, A.W., Pravec, P., 2009. The asteroid lightcurve database. *Icarus* 202, 134–146.
- Yoshida, F., Dermawan, B., Ito, T., et al., 2004. Photometric observations of a very young family-member asteroid (832) karin. *Publ. Astron. Soc. Japan* 56, 1105–1113.
- Yoshida, F., Nakamura, T., 2007. Subaru main belt asteroid survey (SMBAS) — size and color distributions of small main-belt asteroids. *Planet. Space Sci.* 55, 1113–1125.
- Zappalà, V., Cellino, A., Barucci, A.M., et al., 1990. An analysis of the amplitude-phase relationship among asteroids. *Astron. Astrophys.* 231, 548–560.